[26]The probability of spin exchange in the afterglow period may be somewhat greater than in an active discharge. However, the question is probably academic because there can be little doubt that the only electron-producing reaction in the afterglow ($He^M + He^M \rightarrow He + He^+ + e^-$) leaves the typical electron already spin polarized.

[27]J. A. Simpson and L. Marton, Rev. Sci. Instr. 32, 802 (1961); J. Kessler and H. Lindner, Z. Angew. Phys. 18, 7 (1964).

[28]The accelerating column and associated resistor chain were provided through the courtesy of Texas Nuclear Corp., Austin, Tex.

[29]H. A. Tolhoeck, Rev. Mod. Phys. 28, 277 (1956).

[30]N. F. Mott, Proc. Roy. Soc. (London) A124, 425 (1929).

[31]J. van Klinken, Nucl. Phys. 75, 163 (1966).

[32]L. Mikaelyan, A. Borovoi, and E. Denisov, Nucl. Phys. 47, 328 (1963).

[33]S. R. Lin, Phys. Rev. 133, A965 (1964).

[34]G. Holzworth and H. J. Meister, Nucl. Phys. 59, 56 (1968).

[35]K. Jost and J. Kessler, Z. Physik 195, 1 (1966); the plus sign in their paper is in error.

[36]J. Kessler (private communication).

[37]Pressure measurements are accurate to ±20%.

[38]The question of whether or not the collision of spin-oriented $2\,^3S_1$ metastables with a metal surface will produce a spin-polarized electron is being investigated in a separate experiment.

[39]W. A. Fitzsimmons, M. A. thesis (Rice University, 1966) (unpublished).

[40]P. A. Burke, in *Fifth International Conference on the Physics of Electronic and Atomic Collisions: Abstracts of Papers*, edited by I. P. Flaks (Nauka, Leningrad, 1967).

[41]The highest discharge intensity attainable at 0.035 torr with available excitation sources corresponded to 8% absorption of the pumping light.

[42]L. D. Schearer (private communication).

[43]An optical technique has been reported recently for measuring spin dependence of Penning reactions in which X^+ is produced in an electronically excited state. See L. D. Schearer, Phys. Rev. Letters 22, 629 (1969).

[44]N. D. Stockwell, Ph. D. thesis (Rice University, 1967) (unpublished).

PHYSICAL REVIEW A VOLUME 5, NUMBER 1 JANUARY 1972

Direct Demonstration of Spin-Angular-Momentum Conservation in the Reaction $He(2\,^3S_1) + He(2\,^3S_1) \rightarrow He(1\,^1S_0) + He^+ + e^-$ †

J. C. Hill,* L. L. Hatfield, ‡ N. D. Stockwell, § and G. K. Walters
Department of Physics, Rice University, Houston, Texas 77001
(Received 21 June 1971)

Conservation of spin angular momentum in the reaction $He(2\,^3S_1) + He(2\,^3S_1) \rightarrow He(1\,^1S_0) \rightarrow He^+ + e^-$ is demonstrated quantitatively in the afterglow of a helium discharge by measuring the dependence of the electron production rate upon $2\,^3S_1$ spin-state populations, which are manipulated by an optical-pumping technique.

I. INTRODUCTION

The combined use of microwave diagnostic techniques and optical pumping in He^3 has made possible a quantitative demonstration of the conservation of electron spin angular momentum in the reaction

$$He(2\,^3S_1) + He(2\,^3S_1) \rightarrow He(1\,^1S_0) + He^+ + e^- \qquad (1)$$

occurring in the afterglow of a pulsed helium discharge.

Violations of spin conservation in inelastic reactions involving nF states of He are known to occur and are explained in terms of the failure of the LS coupling approximation.[1] Nevertheless, in the preceding paper McCusker *et al.*[2] invoke spin-angular-momentum conservation to account for measured spin polarization of electrons produced by reaction (1) in He^4, and the present work independently confirms the validity of their assumption.

As a direct consequence of the conservation of spin angular momentum the cross section associated with Eq. (1) should depend in a predictable manner on the magnetic spin-states of the reactant $2\,^3S_1$ metastable atoms. Optical pumping is used to control the spin-state populations in the afterglow of a pulsed helium discharge, and microwave diagnostics are used to detect the corresponding change in the number density of electrons produced by the reaction. Since the various reactions in a helium afterglow are well understood, simple, and few in number, the resulting demonstration of spin-angular-momentum conservation is quite direct and unambiguous.

II. THEORY OF EXPERIMENT

This experiment examines reactions occurring in room-temperature high-purity He^3 gas at a pressure of about 2 torr, in the afterglow periods following a repetitively pulsed electrical discharge. Upon termination of the discharge, all of the excited atoms present decay to the ground state within a time of the order of 10^{-7} sec, except for those

in metastable $2\,^1S_0$ and $2\,^3S_1$ states. Ions and electrons remaining from the active discharge are driven to the container walls through enhanced ambipolar diffusion, by terminating the discharge with a 150 μsec burst of rf power that is insufficient to sustain the discharge but sufficient to heat the electrons appreciably. Thus, at the beginning of the afterglow period, the only remaining species of significance in the sample are ground-state helium atoms ($1\,^1S_0$) and singlet ($2\,^1S_0$) and triplet ($2\,^3S_1$) metastable atoms.

Collisions which produce electrons during the afterglow period are, in addition to reaction (1),

$$\mathrm{He}(2\,^1S_0)+\mathrm{He}(2\,^1S_0)\rightarrow \mathrm{He}(1\,^1S_0)+\mathrm{He}^+ + e^- , \qquad (2)$$

$$\mathrm{He}(2\,^1S_0)+\mathrm{He}(2\,^3S_1)\rightarrow \mathrm{He}(1\,^1S_0)+\mathrm{He}^+ + e^- , \qquad (3)$$

all of which occur with cross sections of approximately 10^{-14} cm^2.[3,4] In addition, there is a conversion of singlets to triplets during the afterglow by the reaction

$$\mathrm{He}(2\,^1S_0)+e^-\rightarrow \mathrm{He}(2\,^3S_1)+e^- + 0.79\ \mathrm{eV} \qquad (4)$$

between singlet metastables and thermalized electrons from reactions (1)–(3).[4]

The rate equations governing loss and production of electrons by metastable-metastable collisions in the discharge afterglow are

$$\frac{\partial T}{\partial t} = D_T\nabla^2 T - 2\beta(\{n_i\})\,T^2 - 2\gamma ST + \alpha NS , \qquad (5)$$

$$\frac{\partial S}{\partial t} = D_S\nabla^2 S - 2\xi S^2 - 2\gamma ST - \alpha NS , \qquad (6)$$

$$\frac{\partial N}{\partial t} = D_e\nabla^2 N + \beta(\{n_i\})T^2 + 2\gamma ST + \xi S^2 , \qquad (7)$$

where T, S, and N are triplet, singlet, and electron number densities, respectively; D_T, D_S, and D_e are their respective diffusion coefficients; and β, ξ, γ, and α are the rate coefficients for reactions (1), (2), (3), and (4), respectively. Volume loss of metastables by collisions with ground-state atoms is negligible at the low densities employed,[4,5] and ion-electron recombination occurs at the container walls.

Conservation of spin angular momentum should be reflected through a dependence of the cross section for (1) upon the magnetic quantum numbers m_j of the reactant $2\,^3S_1$ atoms. If $m_j=+1$ (or -1) for both reactant atoms, then the reaction cannot in fact proceed (zero cross section) if spin angular momentum is conserved because the maximum possible total spin projection of the products is one. The reaction can proceed for all other combinations of the reactant m_j's, and for lack of any information on the subject we make the simplest possible assumption here that the cross sections are equal for all such allowed reactions. Thus the rate coefficient $\beta(\{n_i\})$ will depend in a calculable manner upon the distribution of $2\,^3S_1$ atoms among the available sublevels $m_j=+1$, 0, and -1, where $\{n_i\}$ denotes their populations n_+, n_0, and n_-, respectively. Since it is precisely the ratios $n_+:n_0:n_-$ that can be manipulated by the optical-pumping technique, the temporal development $N(t,\{n_i\})$ of electron density in the afterglow period will be a function of $\{n_i\}$. [It is apparent that reactions (2) and (3)—hence ξ and γ—are independent of $\{n_i\}$ since $m_j(2\,^1S_0)\equiv 0$.]

Equations (5)–(7) were solved numerically, under the assumption of spin-angular-momentum conservation, for lowest-mode diffusion and the resulting $N(t,\{n_i\})$ compared with experimental values obtained by microwave methods to be described below. The solutions were obtained by employing the Runge-Kutta method[6] and standard computational techniques. Appropriate diffusion coefficients for metastable atoms and rate coefficients for reactions (1)–(4) were obtained from the literature and adjusted to the pressures and temperatures involved in the experiment. These are listed in Table I. Values for the metastable densities T_0 and S_0 at the beginning of the afterglow period were obtained from measurements of optical absorption at 1.08 μ and 2.06 μ resulting from $2\,^3S$-$2\,^3P$ and $2\,^1S$-$2\,^1P$ transitions, respectively.[7] It was found that $T_0\approx 3S_0$ in accordance with their associated statistical weights.

Since the electrons produced by reactions (1)–(3) have an average initial energy of 9 eV,[8] it was not considered safe to assume that the afterglow electrons are thermalized. Further, conversion of a small fraction of atomic to molecular ions of significantly greater diffusion coefficient can be ex-

TABLE I. Collision and diffusion parameters adjusted to experimental conditions and used in the solution of Eqs. (5)–(7).

Diffusion coefficients (p = sample pressure)

$D_T p = 470$ cm^2 sec^{-1} torr (Ref. 4),
$D_S p = 440$ cm^2 sec^{-1} torr (Ref. 4),
$D_+ p = 460$ cm^2 sec^{-1} torr (for He$^+$ ions).[a]

Reaction rates

$\gamma = \xi = \sigma_1\bar{v}$; $\sigma \simeq 10^{-14}$ cm^2 (Ref. 3).

Average relative velocity $\bar{v} = 1.8\times10^5$ cm sec^{-1} for metastable-metastable collisions at 300 °K;

$\alpha = \sigma_2\bar{v}_e$; $\sigma = 3\times10^{-14}$ cm^2 (Ref. 4);

$\bar{v}_e = 1.6\times10^7$ cm sec^{-1} for e^--metastable collisions at $T_e = 660$ °K.

Lowest-mode diffusion length

$\Lambda_0 = 0.79$ cm.

[a] E. W. McDaniel, *Collision Phenomena in Ionized Gases* (Wiley, New York, 1964), p. 516.

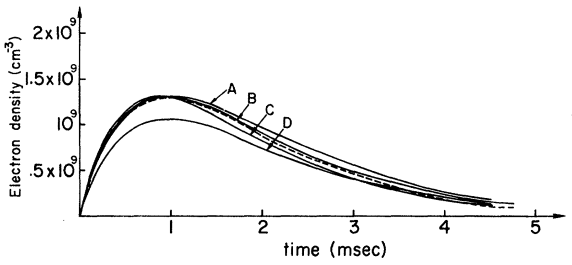

FIG. 1. Electron density vs time in helium afterglow for 1.3% absorption of 1.08-μ light (He^4 lamp on 2 torr He^3 sample). Broken curve represents experimental data. Solid curves represent numerical solutions to Eqs. (5)–(7) for different metastable densities and electron temperatures.
A: $S_0=1.22\times10^{10}$ cm^{-3}, $T_0=3.66\times10^{10}$ cm^{-3}, $T_e=580$ °K;
B: $S_0=1.25\times10^{10}$ cm^{-3}, $T_0=3.75\times10^{10}$ cm^{-3}, $T_e=660$ °K;
C: $S_0=1.32\times10^{10}$ cm^{-3}, $T_0=3.96\times10^{10}$ cm^{-3}, $T_e=840$ °K;
D: $S_0=1.12\times10^{10}$ cm^{-3}, $T_0=3.36\times10^{10}$ cm^{-3}, $T_e=660$ °K.

pected at the 2-torr sample pressures employed. The electron diffusion coefficient D_e is dependent upon both of these factors. Hence it was determined empirically from the experimental data by choosing that value of D_e, in solving the rate equations (5)–(7), that provides the best fit to the experimentally determined $N(t)$. This determination was made in the absence of optical pumping, and lowest-mode diffusion was assumed. Through the relation[9]

$$D_e = D_+(1+T_e/T_g)\,, \tag{8}$$

where D_+ is the free-ion diffusion coefficient (see Table I), we deduce $T_e \approx 660$ °K for the electron "temperature" for a sample-gas temperature $T_g \approx 300$ °K, assuming the ions are predominantly atomic. (Actually since only D_e, and not D_+ or T_e, appears in the rate equations, it is inconsequential whether or not ion conversion is partially responsible for the experimentally determined D_e.) Figure 1 shows the computed fit to $N(t)$ in the absence of optical pumping for several values of T_e, and also illustrates the sensitivity of the fit to T_0 and S_0. Added confidence in the procedure for determining D_e and T_e is provided by the agreement between measured T_0 and S_0 values and the values required for the best fit to the $N(t)$ data.

We now return to the predicted dependence of $\beta(\{n_i\})$ and $N(t, \{n_i\})$ upon $\{n_i\}$. Optical pumping can enrich the population of one of the three m_j levels at the expense of the others. The process is amply discussed in the literature[10–12]; its physical basis is the transfer of angular momentum from circularly polarized pumping radiation to the system of $2\,^3S_1$ atoms through excitation of $2\,^3S$-$2\,^3P$ transitions with selection rule $\Delta m_j = +1$ (or -1) for right (left) circular polarization. The subsequent $2\,^3P$-$2\,^3S$ decay is random with respect to spin orientation so that a net enhancement of appropriate high- (or low-) m_j sublevel populations of the initial level is achieved.

The rate coefficient for the ionizing collision (1) of two triplet metastable atoms, $\beta(\{n_i\})$, can be expressed as a fraction of the rates $\gamma = \xi$ under the aforestated assumption that all spin-allowed cross sections are equal:

$$\beta(\{n_i\}) = [(n_t^2 - n_+^2 - n_-^2)/n_t^2]\gamma, \tag{9}$$

where $n_t = n_+ + n_0 + n_-$ and $(n_+ + n_+)$ and $(n_- + n_-)$ collisions have zero cross sections for reaction (1) under the assumption of conservation of spin angular momentum.

For practical reasons the experiment actually was performed using the rare He^3 isotope with nuclear spin $I = \frac{1}{2}$, rather than with He^4. In this case metastability exchange collisions between $2\,^3S_1$ and $1\,^1S_0$ helium atoms lead to nuclear spin polarization of the far more numerous (factor $\sim 10^6$) He^3 ground-state atoms. Colegrove *et al.* have shown that a "flywheel" effect results in that the exchange collisions provide a tight coupling of the $2\,^3S_1$ m_j sublevel populations to the huge ground-state angular momentum reservoir.[12] Thus $\{n_i\}$ remains constant throughout the afterglow period and is directly calculable in terms of the ground-state nuclear polarization

$$P = [\eta(\uparrow) - \eta(\downarrow)]/[\eta(\uparrow) + \eta(\downarrow)]\,,$$

where the $\eta(\uparrow)$ and $\eta(\downarrow)$ are the $1\,^1S_0$ nuclear spin-state populations corresponding to $m_I = +\frac{1}{2}$ and $-\frac{1}{2}$, respectively. Thus $\beta(\{n_i\})$ becomes $\beta(P)$. The six $2\,^3S_1$ sublevels of He^3 correspond to eigenfunctions $|F, m_F\rangle = |\frac{3}{2}, -\frac{3}{2}\rangle$, $|\frac{3}{2}, -\frac{1}{2}\rangle$, $|\frac{3}{2}, \frac{1}{2}\rangle$, $|\frac{3}{2}, \frac{3}{2}\rangle$, $|\frac{1}{2}, -\frac{1}{2}\rangle$, $|\frac{1}{2}, \frac{1}{2}\rangle$, where $F = I + S'$, and $S' = 1$ is the electron spin quantum number; we denote the populations of these states as n_1 through n_6, respectively. Colegrove *et al.*[12] have shown that the relations between the n_i's and the ground-state nuclear polarization P are

$$\frac{n_1}{n_2} = \frac{n_2}{n_3} = \frac{n_3}{n_4} = \frac{n_5}{n_6} = \frac{1-P}{1+P} \tag{10}$$

and $n_2 = n_5$, $n_3 = n_6$, $T = \sum_{i=1}^{6} n_i$. Further, P is equal to 0.45 ± 0.05 times the difference between the measured fractional absorption of pumping radiation by the sample in polarized and depolarized conditions, respectively.[12–14] Thus P is accessible experimentally, and there remains only the derivation of the expression for $\beta(\{n_i\}) = \beta(P)$. Toward this end it is important to note that the nucleus is merely a spectator in reaction (1). Consequently, the $|F, m_F\rangle$ eigenfunctions may be expanded in terms of $|m_I, m_{s'}\rangle$ functions and the squares of the Clebsch-Gordan coefficients weighted with the associated n_i's gathered on values of $m_{s'} = +1$, 0, and -1. This relates

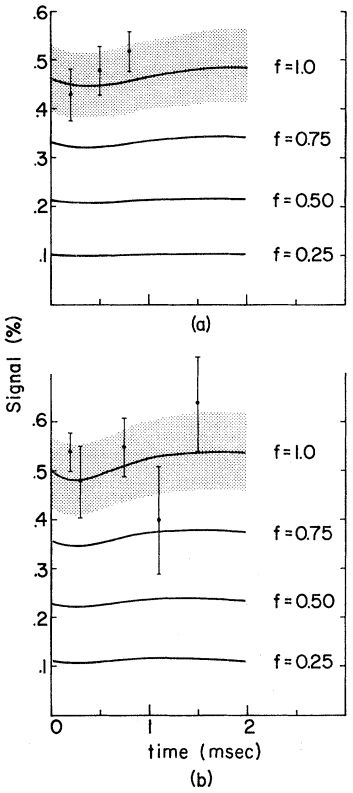

FIG. 2. Anticipated electron density change measured in terms of cavity-shift signal vs time in helium afterglow, and experimental data indicating electron spin conservation. Solid lines indicate predicted signals for 100, 75, 50, and 25% spin conservation computed at the measured values of polarization. Hatched area indicates experimental uncertainty in the polarization measurement for 100% spin conservation. (a) 2% absorption of 1.08-μ light, $P=7.8\%$; (b) 2.6% absorption, $P=8.1\%$.

the six He^3 substrate populations to the effective populations n_+, n_0, and n_-:

$$n_+ = \tfrac{2}{3}n_6 + n_4 + \tfrac{1}{3}n_3 ,$$
$$n_0 = \tfrac{1}{3}n_6 + \tfrac{1}{3}n_5 + \tfrac{2}{3}n_3 + \tfrac{2}{3}n_2 , \qquad (11)$$
$$n_- = \tfrac{2}{3}n_5 + \tfrac{1}{3}n_2 + n_1 .$$

Combining (9)–(11), we obtain finally

$$\beta(P) = \gamma(7 - 6P^2 - P^4)/(9 + 6P^2 + P^4) . \qquad (12)$$

This expression for $\beta(P) = \beta(\{n_i\})$ is substituted into Eqs. (5) and (7), which, together with (6) are solved simultaneously for $S(t, P)$, $T(t, P)$, and $N(t,P)$ by numerical methods with the polarization P as a parameter. All other quantities in the rate equations are specified as outlined previously. The function computed for comparison with experiment is the fractional change

$$[N(t, 0) - N(t, P)]/N(t, 0) \qquad (13)$$

in electron density when a sample of known polarization is depolarized by application of an rf magnetic field that saturates the $1\,^1S_0$ nuclear Zeeman transitions. This function is plotted along with the experimental data in Figs. 2. The hatched area, which reflects uncertainties in the measurement of P, delimits the range of the anticipated experimental result under the assumption that spin angular momentum is fully conserved in reaction (1). Spin nonconservation would yield a null result. For purposes of comparison, predicted values of (13) for conservation of spin angular momentum in only a fraction f of metastable-metastable collisions were calculated by modifying $\beta(P)$:

$$\beta'(P) = \gamma\,[(1+f) + f(7 - 6P^2 - P^4)/(9 + 6P^2 + P^4)] ; \qquad (13')$$

the results for $f = 0.75$, 0.50, and 0.25 are also shown in Fig. 2. It is important to note that uncertainties in such quantities as the electron distribution in the sample, the reaction rates α, γ, and ξ, and the various diffusion coefficients cancel out to a high order of approximation when the ratio (13) is taken. Thus the measured function is significantly sensitive only to the reaction rate $\beta(P)$ for which Eq. (12) is quite reliable.

III. EXPERIMENTAL APPARATUS AND TECHNIQUES

The experimental apparatus is shown in Figs. 3 and 4. The arrangement for optically pumping He^3 is typical.[12] The quartz sample cell containing the He^3 discharge is formed into a microwave cavity and coupled to a source of microwave radiation so that changes in reflected power can be measured. The cavity resonant frequency shifts when free electrons are present according to the relation[15]

$$\Delta\nu(t, P) = kN(t, P) , \qquad (14)$$

where $k = 540$ cm^3 sec^{-1} for the TE_{011} cavity and lowest-mode electron diffusion.[15] [Note that k cancels in Eq. (13).]

The sample cell is a right circular cylinder 1.9 in. long with a diam of 1.8 in. After elaborate cleaning procedures,[16] the cell was filled with 2-torr He^3. The microwave cavity was formed by mounting the sample cell between a copper mesh screen at one end and a circular plate containing the coupling iris to the waveguide circuitry at the other end. The body of the cavity consisted of copper strips wrapped around the sample cell. The cavity had a Q of ~700 and a resonant frequency (without discharge) of 9227.7 MHz. The wire-screen cavity bottom permitted the transmission of optical-pumping radiation into the cell cavity, and a small hole in the circular top plate allowed the measurement of the transmitted radiation. A 100-kHz oscillator pulsed at 90 Hz with a 35% duty cycle

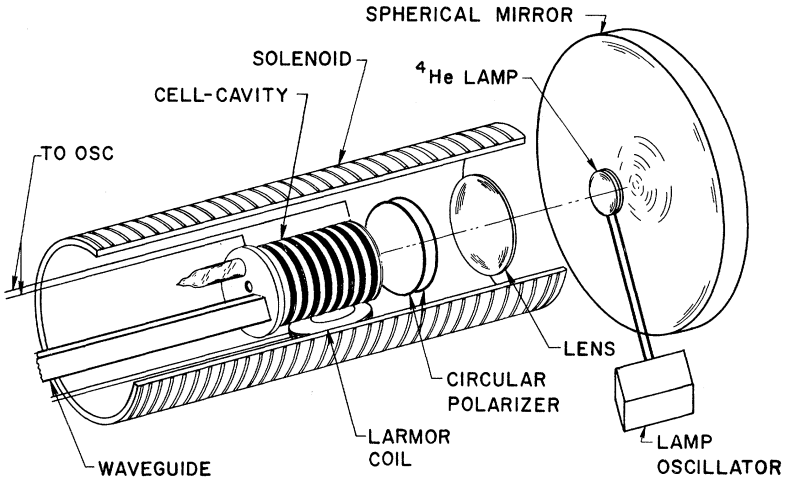

FIG. 3. Diagram of optical-pumping apparatus.

was used to light the discharge in the cell. Precautions were taken to insure that the rf excitation would cut off sharply at the end of a pulse period. In addition, the end of the pulse triggered a 150-μsec burst of rf from a 50-MHz oscillator also connected to the cell. As mentioned above, this short pulse was sufficient to heat the discharge electrons appreciably, enhancing their diffusion to the walls, yet insufficient to relight the discharge. The solenoid, He^4 lamp, circular polarizer, and depolarizing Larmor coil are customary optical-pumping components described elsewhere.[12] The Larmor coil is used to depolarize the $1\,^1S_0$ ground-state nuclear magnetic resonance, and the $2\,^3S_1$ atoms are in turn rapidly ($\sim 10^{-6}$ sec) depolarized by metastability exchange reactions.

The microwave circuit shown in Fig. 4 is straightforward and uses standard X-band components. The 150 μW of power used to probe the cavity had no measurable effect on polarization or electron density. With the screen and iris plate insulated from the cavity body, modes other than the TE_{011} had extremely low Q.

The shift in cavity resonance expected if spin conservation holds, when the cavity is depolarized by saturation of the $1\,^1S_0$ Zeeman transitions, was sought by means of sensitive microwave diagnostic techniques developed by Weaver and Freiberg[17] (Fig. 4). Microwave power reflected from the sample cavity is monitored with a square-law detec-

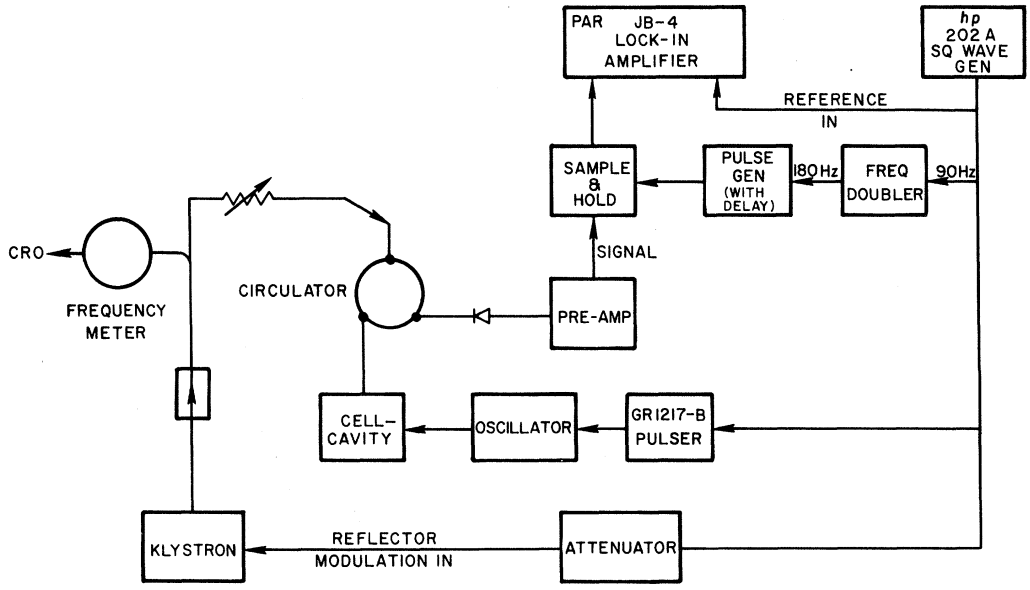

FIG. 4. Block diagram of microwave measurement and sampling apparatus.

tor. The klystron probing frequency is offset from the resonant frequency which the cavity manifests when no electrons are present by such an amount that the cavity acts as a discriminator. Thus a change in reflected power, hence in detector output voltage, is proportional to the change in cavity resonant frequency, which in turn is proportional to the change in number density of electrons in the cavity [Eq. (14)]. In the afterglow period the varying density of electrons causes the cavity resonant frequency to shift in time. Therefore at a given instant the shift in detector voltage relative to the voltage when no electrons are present is directly proportional to the electron number density in the cavity at that instant.

In order to take advantage of the signal-to-noise enhancement afforded by synchronous phase-lock detection, an electronic sampling procedure is used to convert the change in reflected power at a given instant of time in the pulse cycle into an ac signal. The detector output is sampled twice during each pulse cycle, once at a time of interest in the afterglow period and once for reference at a time late in the afterglow when essentially no free electrons are present. This produces a train of signal pulses of alternating height. A sample-and-hold device (Redcor 770-708) is employed to stretch each pulse, maintaining its height until arrival of the succeeding pulse. The result is a signal suitable for synchronous processing: a square-wave train with frequency equal to that of the pulsed discharge and amplitude proportional to the electron density in the cavity at the sampling point.

In actual practice the above procedure is modified in the following manner. The reflector voltage on the klystron is square-wave modulated synchronously with the discharge pulsing so that the probing frequency shifts by such an amount as to give the same detector output voltage at the afterglow sampling time as at the reference time. The resulting null "signal" can be greatly amplified without overloading the electronics. When the

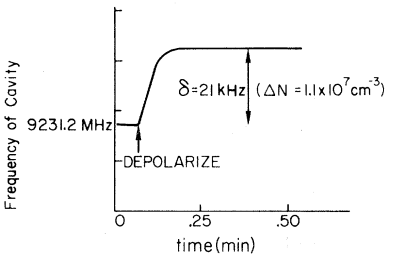

FIG. 5. Typical shift signal showing the change in cavity frequency upon depolarization of $1\,^1S$ nuclei. Sampling time: 0.87 msec into afterglow; polarization = 8.5%; 1.08-μ absorption = 2.5%; predicted signal, $[N(t, P) - N(t, 0)]/N(t, 0) = 0.51\%$; measured signal: 0.60%.

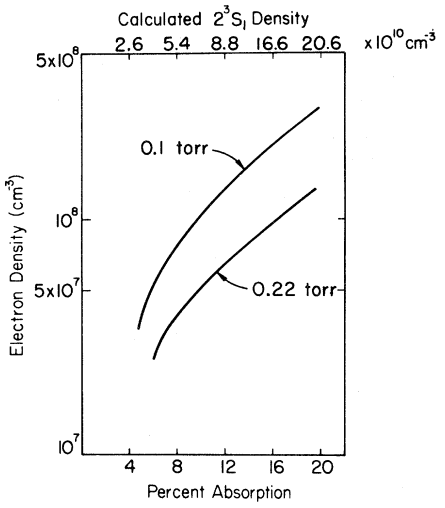

FIG. 6. Measured electron density vs absorption of 1.08-μ light (He^4 lamp on He^4 sample) in active He^4 discharges at two pressures, 0.1 and 0.22 torr.

sample is depolarized the additional free electrons shift the cavity resonance at the sampling time so that the detector outputs at sampling and reference times are unbalanced by an amount proportional to $N(t, 0) - N(t, P)$. The signal function (13) at the sampling time is obtained upon division by the total shift in cavity resonance frequency from its $N = 0$ value. The measurement was made for several sampling points in the afterglow period and for two different values (0.078 and 0.081) of the polarization P. Since the technique was extremely sensitive, care was taken to insure that the signal was not the result of electrical transients, e.g., those which might be introduced by any of the switching operations. A typical signal obtained upon depolarization of the sample is shown in Fig. 5.

IV. RESULTS AND CONCLUSIONS

Experimental values of shift signals are shown in Fig. 2, which also shows the predicted region of signal for 100% conservation of spin angular momentum (hatched area). The presence of any signal under the conditions of this experiment results from the conservation of electron spin projection in the collisions of helium triplet metastable atoms. The agreement with theory demonstrates within 90% confidence limits that the component of spin angular momentum along the quantization axis is fully conserved in reaction (1) to within 10% [i.e., $f \geq 0.90$ in Eq. (13′)].

In a subsidiary experiment, the electron densities in an active steady-state discharge in He^4 were measured because of their importance in the interpretation of the polarized electron beam experiment described in the preceding paper by McCusker, Hat-

field, and Walters.[2] Figure 6 shows the measured electron densities vs 2^3S_1 density (a quantitative measure of the intensity of the discharge) for He^4 sample pressures of 0.1 and 0.22 torr. Under sample conditions closely approximating those employed and analyzed by McCusker *et al.* (8% absorption of He^4 pumping light on He^4 sample and pressure of 0.1 torr) in extracting an optimum polarized electron beam, the electron density is approximately 7×10^7 cm^{-3}. However, the error could be as large as a factor of 2, primarily because of uncertainty in the proportionality constant k in Eq. (14), taken here to be 230 $cm^3\,sec^{-1}$ appropriate to a uniform electron distribution.

†Based on a Master of Arts thesis by J. C. Hill (Rice University, 1969). Work supported in part by U. S. Atomic Energy Commission.

*Present address: Physics Department, Duquesne University, Pittsburgh, Pa. 15219.

‡Present address: Physics Department, Texas Tech University, Lubbock, Tex. 79409.

§Present address: Aerospace Corporation, San Bernadino, Calif. 92401.

[1]C. C. Lin and R. G. Fowler, Ann. Phys. (N. Y.) 15, 461 (1961).

[2]M. V. McCusker, L. L. Hatfield, and G. K. Walters, preceding paper, Phys. Rev. A 5, 177 (1972). See also M. V. McCusker, L. L. Hatfield, and G. K. Walters, Phys. Rev. Letters 22, 817 (1969).

[3]M. A. Biondi, Phys. Rev. 88, 660 (1952).

[4]A. V. Phelps, Phys. Rev. 99, 1307 (1955).

[5]A. V. Phelps and J. P. Molnar, Phys. Rev. 89, 1202 (1953).

[6]D. D. McCracken and W. S. Dorn, *Numerical Methods and Fortran Programming* (Wiley, New York, 1964), p. 317.

[7]A. C. G. Mitchell and M. W. Zemansky, *Resonance Radiation and Excited Atoms* (Cambridge U.P., Cambridge, England, 1961), Chap. 3.

[8]J. C. Ingraham and S. C. Brown, Phys. Rev. 138, A1015 (1965).

[9]S. C. Brown, *Introduction in Electrical Discharges in Gases* (Wiley, New York, 1966), p. 61.

[10]F. D. Colegrove and P. A. Franken, Phys. Rev. 119, 680 (1960).

[11]L. D. Schearer, *Advances in Quantum Electronics* (Columbia U.P., New York, 1961), pp. 239–251.

[12]F. D. Colegrove, L. D. Schearer, and G. K. Walters, Phys. Rev. 132, 2561 (1963).

[13]R. C. Greenhow, Phys. Rev. 136, A660 (1964).

[14]This relation holds only for $P \ll 1$, a condition satisfied in the present experiment.

[15]H. J. Oskam, Philips Res. Rept. 13, 335 (1958).

[16]W. A. Fitzsimmons, L. L. Tankersley, and G. K. Walters, Phys. Rev. 179, 156 (1969).

[17]L. A. Weaver and R. J. Freiberg, J. Appl. Phys. 39, 4283 (1968).

PHYSICAL REVIEW A VOLUME 5, NUMBER 1 JANUARY 1972

Polarized Electrons from Photoionization of Polarized Alkali Atoms*

V. W. Hughes, R. L. Long, Jr.,† M. S. Lubell, M. Posner,‡ and W. Raith
Yale University, New Haven, Connecticut 06520
(Received 30 June 1971)

The process of photoionization of polarized alkali atoms in an atomic beam has been studied for potassium and lithium. Depolarization processes associated with photoionization of alkali molecules and optically excited atoms were discovered. After eliminating these depolarization mechanisms, the measured photoelectron polarization agreed within an accuracy of 3% with the predicted polarization based on the current theory for this electric dipole process. Using a polarized Li^6 atomic beam and a pulsed uv light source, we have produced an intense and highly polarized electron beam with 2×10^8 electrons in 1.5 μsec and with a polarization of 0.78, which is a suitable prototype injector source for a high-energy electron accelerator.

I. INTRODUCTION

Investigation of the spin polarization of electrons from atomic systems is a valuable approach to the study of basic atomic processes. In addition, such investigation provides a basis for the development of a source of polarized electrons. One of the earliest proposals for producing polarized electrons was made in 1930 by Fues and Hellman,[1] who suggested that polarized electrons could be obtained from photoionization of a polarized alkali-atom beam. The suggestion was based upon the fact that photoionization is primarily an electric dipole transition, and hence the ejected photoelectrons should have the same polarization as the valence electrons of the alkali atoms. The first attempt to study this process was made in 1961 by Friedmann, who reported obtaining an electron beam of high intensity and high polarization.[2] Friedmann's results, however, could not be reproduced.[3,4]

Our work at Yale was begun with two objectives —the study of the spin-dependent effects in the photoionization of alkali atoms, and the development of a polarized electron source which would be use-